Temperature dependence of the intrastack exchange interaction for a quasi-one-dimensional organic conductor

B. Pongs and E. Dormann
Physikalisches Institut, Universität Karlsruhe, D-76128 Karlsruhe, Germany
(Received 16 August 2001; revised manuscript received 23 October 2001; published 5 April 2002)

The electron spin resonance (ESR) of $(pyrene)_{12}(SbF_6)_7$ is measured as function of crystal orientation for temperatures above and below the Peierls transition temperature $T_P = 116$ K. The principal values of the pyrene g tensor (2.00274, 2.00235, 2.00225) are determined. In spite of a defect concentration amounting to $2-3\times10^{-2}$ per formula unit, the ESR linewidth is below 60 mG in the metallic phase. The temperature dependence of the intrastack exchange interaction between localized defects and conduction electrons is derived. The exchange integral decreases by a factor of 8 between T_P and room temperature.

DOI: 10.1103/PhysRevB.65.144451 PACS number(s): 76.30.Pk, 76.30.Rn, 71.30.+h

I. INTRODUCTION

The temperature dependence of the molecular packing and wave function's overlap of aromatic molecules is currently a topic of reactivated research and fascinating experimental results.[1] We have used quasi-one-dimensional (quasi-1D) organic conductors, built up from radical cations of simple aromatic hydrocarbons (arenes) like perylene and inorganic counterions like PF_6 or SbF_6 as model systems. We showed that the exchange interaction between the mobile π-orbital conduction electrons and the localized intrastack radical defects of typical radical cation salts can be characterized by electron spin resonance (ESR) via a detailed analysis of the orientation and temperature dependence of the ESR linewidth and relaxation rates.[2,3] On the other hand, we could show that the octahedral complex anions are enabled to display fast reorientational (rotational) jumps at room temperature, but that the freezing-in of this motion and the subsequent interstack coupling of arene radical cations via the squeezed-in counterions seem to be a prerequisite for the occurrence of the three-dimensionally ordered static Peierls-distorted phase in quasi-1D conducting radical cation salts.[4–6]

Therefore, for the present ESR analysis, we use the highly 1D organic conductor $(pyrene)_{12}(SbF_6)_7$ [abbreviated $(PY)_{12}(SbF_6)_7$ with $PY = C_{16}H_{10}$], in order to derive the temperature dependence of the intrastack exchange interaction, which reflects the variation of the π-molecular-orbital wave function's overlap along the stacking direction caused by thermal lattice expansion and, most of all, increasing librational amplitude. Pyrene radical cation salts are uniquely qualified for this analysis, because different packing rules are realized in their 1D-pyrene stacks: 0° as well as 60° stacking and even 60° reorientational jumps for varied temperature.

We proved already that the 12:7 stoichiometric salt is especially appropriate for such kind of analysis, because it is an especially anisotropic one-dimensional conductor (i.e., $\sigma_\parallel/\sigma_\perp \approx 10^4$:1, close to T_P), with a Peierls transition temperature of only $T_P = 116$ K, but considerably larger respective molecular field temperature $T_{MF} = 290$ K (Ref. 7) (Fig. 1). Thus a comparably large temperature range between T_P and room temperature is left for the derivation of the exchange integral's temperature dependence. In addition, we proved the absence of solvent molecules and neutral arenes in this 12:7 salt by means of high-resolution solid-state nuclear magnetic resonance.[8] Last but not least, we demonstrated the freezing-in of the SbF_6 rotational motion on approach to the Peierls transition T_P.[6] Our report is organized as follows: After presenting the experimental techniques and results in Sec. II and the model assumptions and adopted quantitative relations in Secs. III A and III B, we analyze the ESR results in Sec. III C. We have to distinguish the low-temperature range with predominating localized defects, the transition region with increasing exchange and motional narrowing of the hyperfine and defect-spin conduction-electron

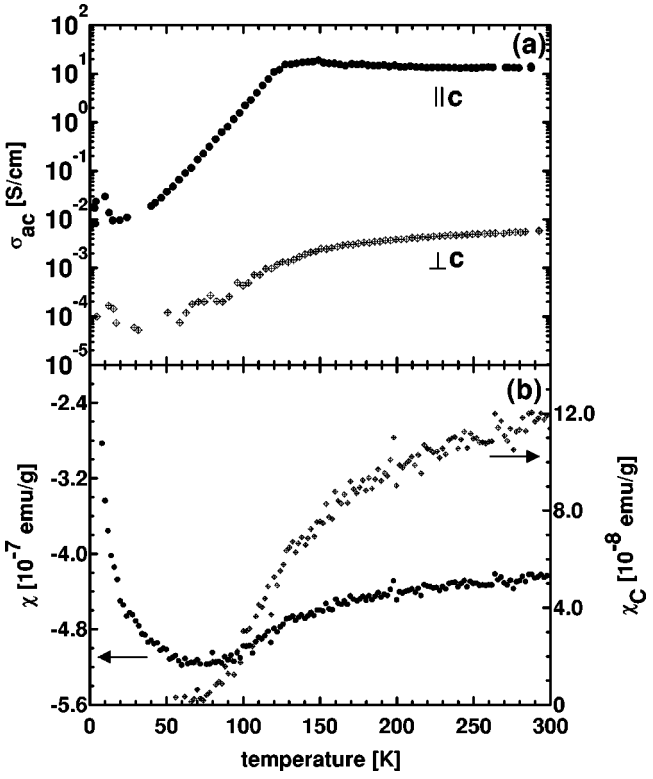

FIG. 1. Microwave conductivity parallel and perpendicular to the stacking direction c (a) and total and conduction-electron part of magnetic susceptibility (b) of $(PY)_{12}(SbF_6)_7$.

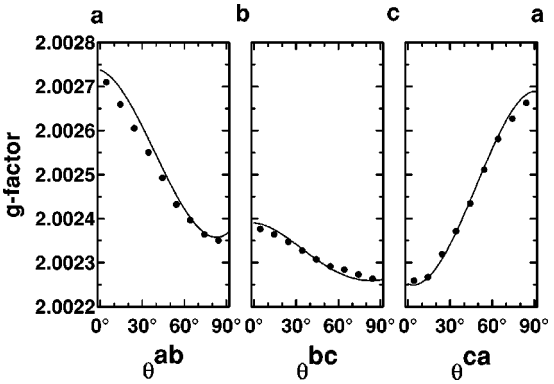

FIG. 2. g-factor of $(PY)_{12}(SbF_6)_7$in three perpendicular planes at room temperature. The solid lines are fits of Eq. (1).

spin dipolar interactions (giving rise to anisotropic ESR-line-broadening contributions), and the ''metallic'' range, giving access to the temperature dependence of the exchange interaction. Our main conclusions are summarized in Sec. IV.

II. EXPERIMENTAL DETAILS AND RESULTS

A. Crystal growth

$(PY)_{12}(SbF_6)_7$ crystals were grown by anodic oxidation in a three-compartment cell at $T=0°C$ using platinum electrodes. Therefore 600 mg of zone-refined pyrene and 1400 mg of Bu_4NSbF_6 were dissolved in 60 ml dichloromethane (CH_2Cl_2). With a constant voltage of 2.6 V applied for 24–72 h, leading to a current of approximately 70 μA, black platelike crystals were obtained.

B. Electron spin resonance

1. g tensor

All ESR measurements were performed on a BRUKER ESP 300E spectrometer at 9.45 GHz (X Band). The field-frequency lock technique of the spectrometer allows measurements of the g value with a relative accuracy of $\pm 5 \times 10^{-6}$. Absolute values of the g factor were obtained by calibration with a $(\text{fluoranthene})_2PF_6$ crystal. To determine the principal values of the g tensor we measured the angular dependence of the g factor in three perpendicular planes at room temperature (Fig. 2). The angular dependence of the g factor for magnetic fields in the ab plane follows the formula[9]

$$g^2(\theta^{ab}) = (g_{aa}\cos\theta^{ab} + g_{ab}\sin\theta^{ab})^2 + (g_{ab}\cos\theta^{ab} + g_{bb}\sin\theta^{ab})^2 + (g_{ac}\cos\theta^{ab} + g_{bc}\sin\theta^{ab})^2. \quad (1)$$

g_{ij} are the matrix elements of the g tensor in the laboratory system and θ^{ab} is the angle between the laboratory axis and the static magnetic field (Fig. 2). The formula for the ac and bc planes is similar. The principal values of the g tensor for $(PY)_{12}(SbF_6)_7$and their relation to the molecular geometry are listed in Table I. The z direction is equivalent to the c direction of the measurement in Fig. 2. Since this direction shows the smallest g value, it corresponds to the stacking direction of the pyrene molecules as known from other arene radical cation salts.

TABLE I. Principal values of the g tensor of $(PY)_{12}(SbF_6)_7$and other pyrene radical cation salts with stoichiometry $PY_7PY_4X_4 \cdot 4CH_2Cl_2$. The z direction corresponds to the normal direction of the molecular plane as well as the stacking direction of the pyrene molecules; the x and y directions are perpendicular to the stacking direction.

	$(PY)_{12}(SbF_6)_7$	$X=AsF_6$	$X=PF_6$
g_x	2.00274	2.00259	2.00253
g_y	2.00235	2.00242	2.00252
g_z	2.00225	2.00224	2.00226

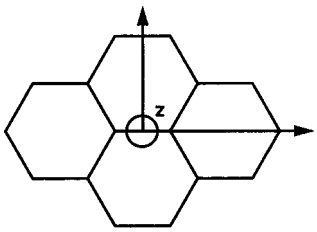

To our knowledge, the g tensor of pyrene radical cations was hitherto not known. The g tensor of $(PY)_{12}(SbF_6)_7$has the largest anisotropy compared to other pyrene radical cation salts[10] (Table I). Enkelmann determined the symmetry of the unit cell of $(PY)_{12}(SbF_6)_7$to $A2/m(a=40.34(4),\ b=14.36(3),\ c=13.70(3),\ \beta=103.0(3)$ (Refs. 11 and 12)], but could not determine the detailed molecular arrangement due to structural defects. Thus neighboring pyrene molecules in the stack can only have the same orientation or must be rotated against each other by an angle of 90° around the stacking direction. Because of the large g anisotropy compared to other pyrene radical cation salts (Table I), the 90° orientation can be excluded. Thus all pyrene molecules in the undisturbed stack have equal orientations, which means that the g tensor of the $(PY)_{12}(SbF_6)_7$salt is equivalent to the g tensor of the individual pyrene molecule. The temperature dependence of the g tensor was analyzed as well.[10]

2. Angular dependence of the electron-spin-resonance linewidth

Measurements of the static magnetic susceptibility (Fig. 1) have shown that there exist typically $2-3\times10^{-2}$ Curie paramagnetic defects per formula unit in our $(PY)_{12}(SbF_6)_7$ crystals.[10,7] Nevertheless, in contrast to the low-temperature behavior of perylene-PF_6 salts,[3] $(PY)_{12}(SbF_6)_7$ shows only one Lorentzian-shaped ESR signal over the whole temperature range between 4.2 K and 290 K, with a linewidth of only about 50 mG at room temperature. Thus there must exist a strong exchange coupling between the defect spins mutually and with the conduction electrons.

The angular dependence of the ESR linewidth (half width on half height of the ESR absorption line) at different temperatures is shown in Fig. 3. The angular dependence at room temperature shows the typical behavior of a dipole-dipole interaction between conduction electrons and intra-

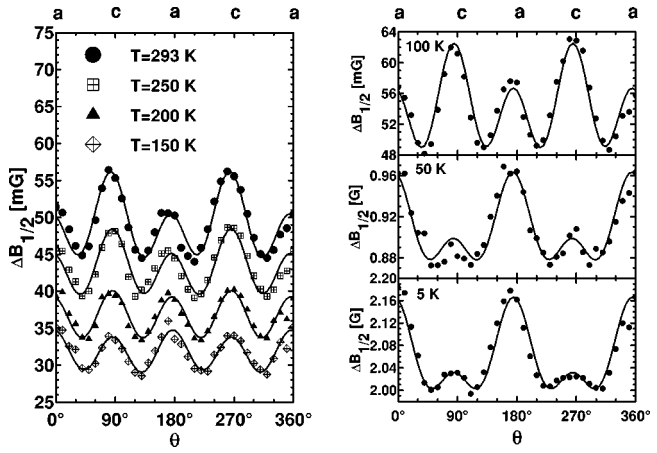

FIG. 3. Angular dependence of the ESR linewidth (X band) in the ac plane of $(PY)_{12}(SbF_6)_7$ at different temperatures. The c direction corresponds to the stacking direction. The solid lines are guides to the eyes.

stack paramagnetic defects: the maximum of the linewidth is observed in the c direction, i.e., in the stacking direction, and the first minimum at the magic angle of 54.7° between the static magnetic field and c direction.

In the temperature range above the Peierls transition (i.e., $T>116$ K, left part of Fig. 3) the absolute value of the linewidth decreases with decreasing temperature, as well as the height of the maximum in the c direction. Both phenomena

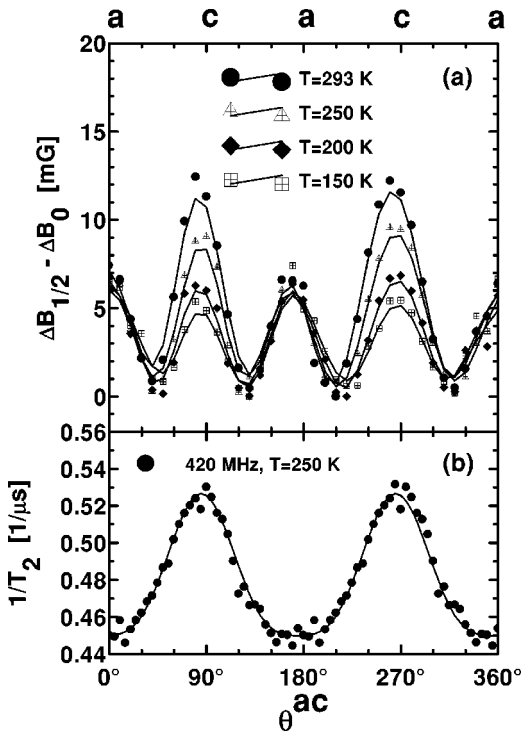

FIG. 4. (a) Frequency-dependent part of the ESR linewidth at X band above T_P. The height of the maximum in the c direction decreases with decreasing temperature, whereas the relative height of the a maximum is not affected by the temperature. (b) Anisotropy of $1/T_2$ at 250 K and 420 MHz (Ref. 13). The solid line shows the fit with formula (2).

can be explained by the temperature dependence of the exchange integral as we will show in Sec. III C 1. In order to distinguish the different contributions to line broadening and exchange or motional narrowing,[2,3] the frequency dependence of the anisotropy of the linewidth had to be analyzed (Fig. 4).

The height of the maximum in the a direction relative to the offset ΔB_0, on the other hand, shows no significant temperature dependence (Fig. 4), though one would expect the same decrease of the height if the angular dependence of the linewidth is only caused by intrastack dipole-dipole interactions. Therefore there must be an additional contribution to the linewidth in the a direction, which probably has its origin in the spatial distribution and anisotropy of g tensors and hyperfine interaction of the paramagnetic defects. At 4.2 K, where the defects dominate the ESR signal because of their Curie-law-like susceptibility, the maximum of the linewidth appears in the a direction. We suppose that this is caused by a distribution of g values of the defects, which results in an ''inhomogeneous'' broadening of the linewidth and has also an influence on the linewidth at higher temperatures, especially in the a direction. The explanation by g variations is further supported by comparison with the angular variation of $1/T_2$ recorded at 420 MHz (Fig. 4), i.e., at 22 times a smaller Zeeman interaction. No secondary maximum in the a direction is observed at the lower frequency.

III. THEORETICAL ANALYSIS

A. Dipole-dipole interaction

The angular dependence of the ESR linewidth due to dipole-dipole interactions between localized spins and conduction electrons in the one-dimensional stack can be described by the expression[3]

$$\Delta B_{1/2}=\Delta B_0+d\left\{\frac{3}{8}(1-3\cos^2\Theta)^2J(0)+\frac{15}{14}\sin^2\Theta\cos^2\Theta J(\omega)+\frac{3}{8}\sin^4\Theta J(2\omega)\right\}. \quad (2)$$

ΔB_0 is an offset caused by the g tensor distribution, hyperfine interaction, and relaxation by the Elliot mechanism, and is, at least in the simplest case, angular independent. d describes the strength of the dipolar coupling and depends primarily on the average distance between the defect spins and the conduction electrons r:

$$d=\frac{\gamma^3\hbar^2S(S+1)}{r^6}.$$

$J(\omega)$ is the spectral density. The assumption of an exponential decay of the correlation between the spins with a correlation time τ leads to

$$J(\omega)=\frac{2\tau}{1+\omega^2\tau^2}.$$

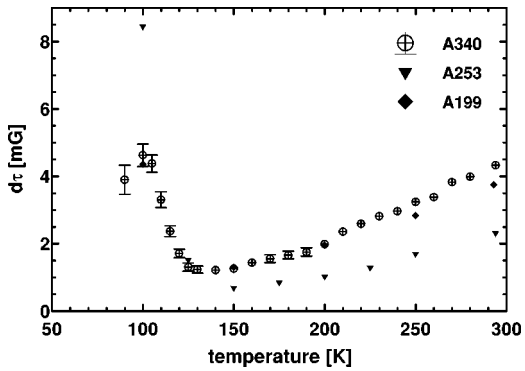

FIG. 5. Temperature dependence of $d\tau$ for three different samples (A199, A253, A340) derived by the fit of Eq. (3) to the measured angular dependences of the ESR linewidths.

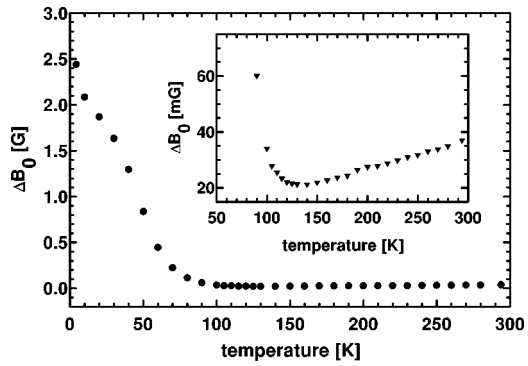

FIG. 6. Temperature dependence of the angular-independent contribution to the ESR linewidth. The inset shows the high-temperature range on an extended scale (with suppressed zero).

Parameters of the fit of Eq. (2) are ΔB_0, d and τ. However, in the X band it is not possible to determine d and τ separately, but only the product $d\tau$, since there is $\omega\tau \gg 1$ and therefore $J(2\omega), J(\omega) \ll J(0)$. Hence, the relevant expression for the X band linewidth is

$$\Delta B_{1/2} = \Delta B_0 + \frac{3}{4} d\tau (1 - 3\cos^2\Theta)^2. \tag{3}$$

To estimate the magnitude of d and τ the angular dependence of the transversal relaxation time $T_2 = 1/(\gamma \Delta B_{1/2})$ of $(PY)_{12}(SbF_6)_7$was measured with pulsed ESR at 420 MHz (Ref. 13) (Fig. 4). At $T = 250$ K $d(250\ \text{K}) = 8.28 \times 10^6$ G/s and $\tau(250\ \text{K}) = 2.61 \times 10^{-10}$ s were obtained. Hence the mean value for the distance between the interacting spins can be calculated to $\langle 1/r^6 \rangle^{-1/6} = 28.6$ Å, about 8.5 times the typical intrastack separation of pyrene radicals and consistent with a statistical distribution of the Curie paramagnetic defects.

The temperature dependence of $d\tau$ for different samples derived from the fit of Eq. (3) to the angular dependences of the ESR linewidth is shown in Fig. 5. Whereas the absolute values vary slightly from sample to sample, which is obvious due to the different concentrations of defects in the samples, the trend of the curves is always the same: $d\tau$ decreases from 290 K to about 125 K and shows then a relative sharp increase down to 90 K. For temperatures below 90 K the dipole-dipole interaction between the conduction electrons and the paramagnetic defects is no longer the dominating reason for the anisotropy of the ESR linewidth because of the dying out of the conduction electrons due to the Peierls transition. Therefore Eq. (3) no longer gives a reasonable fit for the angular dependence of the linewidth. From the angular-dependent measurements of $\Delta B_{1/2}$ we derived also the temperature dependence of ΔB_0. The result is plotted in Fig. 6. As mentioned above ΔB_0 decreases slightly from room temperature down to T_P, as one would expect for relaxation due to the Elliot mechanism[14] or, as we will see in Sec. III C 1, is here due to a temperature dependence of the exchange coupling of conduction electrons and paramagnetic defects. The proof of the latter mechanism is based on the experimental observation that the anisotropy of the ESR linewidth (Fig. 5) decreases more strongly than the linewidth ΔB_0 (Fig. 6). For temperatures below the Peierls transition the linewidth shows a steep rise on account of the gradual loss of conduction electrons which leads to a decrease of motional and exchange narrowing. Instead the ESR signal is at lower temperatures more and more dominated by the localized defects and their hyperfine interaction and g-tensor distribution.

B. Bottleneck model

To receive a correlation between the parameter $d\tau$ and the exchange integral J we revert to a bottleneck model, which was already successfully introduced for fluoranthene and perylene radical cation salts.[3,2,15]

As mentioned above the conduction-electron spins and the defect spins must be coupled by a strong exchange interaction because they contribute both to the same Lorentzian-shaped ESR line. That means that the relaxation between conduction electrons and defects is fast enough to give rise to a detailed balance between the two spin systems before the spins relax to the lattice. The weak coupling to the lattice represents a bottleneck in the relaxation paths of conduction electrons and defects and the mutual relaxation rates obey the familiar detailed-balance relation

$$\left(\frac{1}{T_1}\right)_{DC} \chi_D = \left(\frac{1}{T_1}\right)_{CD} \chi_C . \tag{4}$$

DC and CD label relaxation from defect spins to conduction electrons and vice versa. The correlation time τ used in Eq. (3) is the time during which the dipole-dipole interaction between both spin systems is active and is therefore affected by the relaxation rates as follows:

$$\frac{1}{\tau} = \left(\frac{1}{T_1}\right)_{DC} + \left(\frac{1}{T_1}\right)_{CD} . \tag{5}$$

In the relevant temperature range above 90 K the susceptibility of the conduction electrons is much larger than the defect-spin susceptibility ($\chi_C \gg \chi_D$).[7] Referring to Eq. (4) the second term of Eq. (5) can be neglected. The relaxation of the localized defects to the conduction electrons can be described in analogy to the Korringa relaxation of nuclei in

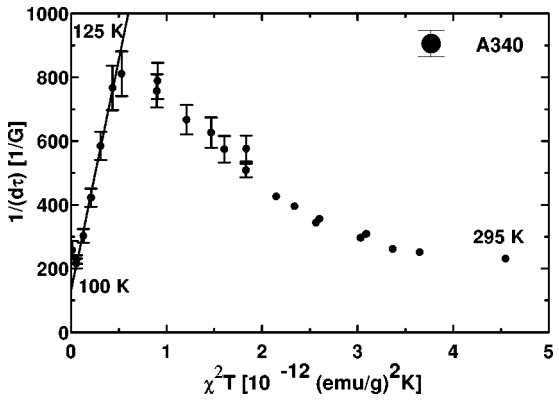

FIG. 7. $1/d\tau$ as a function of $\chi_C^2 T$ for sample A340. The linear correlation for $T \leqslant 125$ K proves that the assumption of temperature independence of $r^6 J^2$ is obeyed in this temperature range.

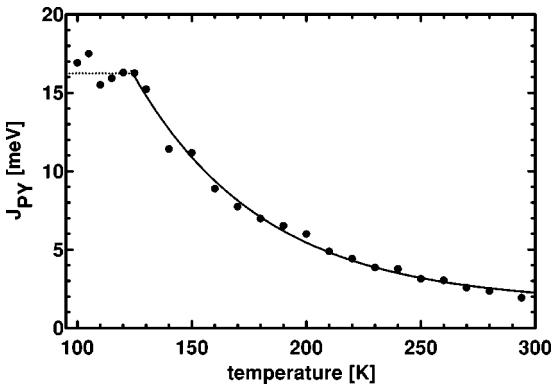

FIG. 8. Temperature dependence of the exchange constant J referring to one pyrene molecule. The solid line is explained in the text (see Sec. III C 2).

metals if one replaces the hyperfine constant a by the exchange constant J in the Korringa law[16]:

$$\frac{1}{\tau} \approx \left(\frac{1}{T_1}\right)_{DC} = \frac{\pi k_B}{\hbar \mu_B^4} J^2 \chi_C^2 T.$$

Investigations of perylene radical cation salts have shown that for a correct description of $d\tau$ a temperature-independent constant term has to be added,[3] leading finally to the following relation between $d\tau$ and J:

$$\frac{1}{d\tau} = \frac{\pi k_B r^6}{\hbar^3 \gamma^3 \mu_B^4 S(S+1)} J^2 \chi_C^2 T + \left(\frac{1}{d\tau}\right)_0. \qquad (6)$$

C. Temperature dependence of the exchange constant

1. Experimental results

In Fig. 7, $1/d\tau$ is plotted as a function of $\chi_C^2 T$. Here χ_C is known from measurements of the static magnetic susceptibility[7] (Fig. 1). Assuming a nearly-temperature-independent J and r, as was found in fluoranthene and perylene radical cation salts[3,2,15] in the temperature range below and around the Peierls transition, there should be a linear relationship between $1/d\tau$ and $\chi_C^2 T$. This condition is as well fulfilled in $(PY)_{12}(SbF_6)_7$between 90 K and 125 K. The linear regression fit in this temperature range yields a value for the temperature independent offset of $(d\tau)_0^{-1} = 129.8\ G^{-1}$. For temperatures above 125 K the assumption of the temperature independence of the exchange constant and of the distance between the interacting spins is evidently not valid. For the temperature dependence of r we made the approach

$$r(T) = r_0(1 + \alpha T).$$

To estimate a value for the relative linear expansion coefficient α along the stacking direction c, we took the measured value for perylene radical cation salts of $\alpha \approx 1 \times 10^{-4}$ 1/K.[5] This leads to an only 10% change in the value of r^6 between 125 K and 295 K. Therefore the deviation from a linear variation for $T > 125$ K of the data points in Fig. 7 is mainly caused by a temperature dependence of J. Since all other parameters in formula (6) are known, this temperature dependence of the exchange constant referring to one pyrene molecule can be calculated from the measured data of $d\tau$. The result is depicted in Fig. 8. $(PY)_{12}(SbF_6)_7$has an exchange constant between conduction electron and defect spin of about 2 meV at room temperature that gets stronger on cooling and reaches finally an approximately 8 times larger constant value of 16.2 meV at 125 K. Since a stronger exchange coupling is synonymous with a smaller ESR linewidth and linewidth anisotropy, the calculated temperature dependence of J is the origin of the linewidth decrease already mentioned in Sec. II B 2.

Compared to the results of the low-temperature analysis performed on fluoranthene radical cation salts, which yields an exchange constant of $J_{FA_2} = 42$–56 meV in the temperature-independent regime $T < T_P$,[2] $(PY)_{12}(SbF_6)_7$ has a smaller exchange constant. This is in accordance to the larger linewidth found in the pyrene salt.

2. Discussion

An explanation for the strong increase of J on approach to the Peierls transition can be based on available information about the freezing-in of molecular motions[6] on approach to the Peierls transition temperature T_P of $(PY)_{12}(SbF_6)_7$.

Generally, a harmonic and an anharmonic contribution of the temperature dependence of $J(T)$ have to be distinguished. The anharmonic part reduces the wave-function overlap between the neighboring molecules via the thermal expansion. Since π-molecular orbitals, built up from carbon p electrons, are responsible for the exchange integral, the related distance dependence is much weaker than, e.g., in $3d$ transition-metal compounds. On the other hand, the harmonic contribution, especially the increase with T of the librational amplitudes of the stacked arene molecules, reduces the π-molecular wave functions' overlap severely.

The solid line in Fig. 8 represents an exponential decrease of the exchange constant with increasing temperature:

$$J(T) = J_0 e^{-\text{const} \times T},$$

which fits the experimental data well. This behavior is known from coherent x-ray scattering in the case of atomic vibrational motion, which leads to a reduction of the diffraction peak intensity by the Debye-Waller factor in an analogous manner. Since the exchange constant J is a measure for the effectivity of intrastack orbital overlap, we assume that primarily librational motion of the pyrene molecules around their rest position weakens the wave-function overlap for temperature increasing from T_P to room temperature. On the other hand, for the locking of a three-dimensional Peierls-distorted phase interstack coupling mechanisms are necessary. We suggested from NMR investigations that such an interstack coupling proceeds via bonding contribution between the H atoms of the pyrene molecules and the F atoms of the hexafluoride anions.[6,17] As long as pyrene molecules or anions are in motion this coupling cannot be established. This is the scenario for $T > T_p$ in the fluctuating regime. On cooling down the amplitude of the librations of the pyrene molecules are reduced (as well as the anion rotations), giving rise to the stronger intrastack exchange coupling constant as well as increased interstack coupling. At 125 K the motion of the pyrene molecules is essentially frozen in, which is reflected by a constant J. Since ^{19}F relaxation-rate measurements prove that the anion rotation slows down on approach to the Peierls transition as well,[6] we conclude that the absence of motion of both the pyrene molecules and the anions is a necessary precondition for the development of an interstack coupling mechanism and hence for the occurrence of the Peierls transition.

IV. CONCLUDING REMARKS

We derived the g tensor, appropriate for pyrene radical cations (Table I). This allows the ESR identification of the pyrene radical molecular orientation in any radical cation salt. The ''localized'' radical defects of the 12:7 stoichiometric pyrene hexafluoroantimonate salt could thus be characterized. The narrowing of the ESR linewidth and anisotropy in the temperature range below and approaching the Peierls transition temperature could be measured and quantitatively described within the familiar bottleneck model established earlier for the radical cation salts. Most importantly, the broadening of the ESR linewidth and the increasing influence of the anisotropic contributions is analyzed for $(PY)_{12}(SbF_6)_7$for temperatures increasing from $T_P = 116$ K up to room temperature. We conclude that the relevant exchange integral decreases in this temperature range by more than a factor of 8. This reflects the reduction of intrastack wave-function overlap, primarily caused by increasing librational amplitudes. The defect-spin conduction-electron spin exchange interaction gives thus an enlarged picture of what is going on in the intact molecular stacks. A decreasing wave-function overlap for increasing temperature resulting in contraction of the conduction-electron bandwidth and corresponding increase of the conduction-electron magnetic susceptibility has been suggested, based on experimental evidence, for perylene radical cation salts in the past.[17] This variation has now been unraveled quantitatively.

ACKNOWLEDGMENTS

We thank I. Odenwald for crystal growth and C. Buschhaus, G. Fischer, A. Kaiser, M. T. Kelemen, S. Matejcek, B. Pilawa, and T. Wokrina for discussions and contributions. This work was financially supported by the Deutsche Forschungsgemeinschaft within the Sonderforschungsbereich 195 (Universität Karlsruhe).

[1] J.H. Schön, C. Kloc, and B. Batlogg, Phys. Rev. Lett. **86**, 3843 (2001).
[2] E. Dormann and G. Sachs, Ber. Bunsenges. Phys. Chem. **91**, 879 (1987).
[3] A. Wolter, U. Fasol, R. Jäppelt, and E. Dormann, Phys. Rev. B **54**, 12 272 (1996).
[4] G. Nemec, V. Illich, and E. Dormann, Synth. Met. **95**, 149 (1998).
[5] C. Buschhaus, R. Moret, S. Ravy, and E. Dormann, Synth. Met. **108**, 21 (2000).
[6] A. Kaiser, B. Pongs, G. Fischer, and E. Dormann, Phys. Lett. A **282**, 125 (2001).
[7] B. Pongs, S. Matejcek, M.T. Kelemen, C. Buschhaus, and E. Dormann, Synth. Met. **120**, 839 (2001).
[8] A. Kaiser, G. Fischer, and E. Dormann, Synth. Met. **124**, 311 (2001).
[9] W. Gordy, *Theory and Applications of Electronspin Resonance* (Wiley Interscience, New York, 1980).
[10] B. Pongs, Ph.D. thesis, Universität Karlsruhe (TH), Germany (2001); *Elektronenspinresonanz an Pyrenradikalkationensalzen* (Shaker Verlag, Aachen, 2001).
[11] V. Enkelmann, Habilitationsschrift, Universität Freiburg, Germany, 1983.
[12] V. Enkelmann, Adv. Chem. Ser. **217**, 177 (1988).
[13] T. Wokrina (private communication).
[14] R.J. Elliot, Phys. Rev. **96**, 266 (1954).
[15] G. Sachs, E. Pöhlmann, and E. Dormann, J. Magn. Magn. Mater. **69**, 131 (1987).
[16] A. Heeger, in *Localized Moments and Non-moments in Metals: The Kondo Effect*, Vol. 23 of *Solid State Physics* (Academic Press, New York, 1969).
[17] R. Desquiotz, M. Hofmann, and E. Dormann, Eur. Phys. J. B **16**, 403 (2000).